



Cite this: *Green Chem.*, 2015, **17**, 3018

Received 10th February 2014,  
Accepted 9th March 2015

DOI: 10.1039/c4gc00219a  
[www.rsc.org/greenchem](http://www.rsc.org/greenchem)

## Continuous catalytic upgrading of ethanol to *n*-butanol and >C<sub>4</sub> products over Cu/CeO<sub>2</sub> catalysts in supercritical CO<sub>2</sub>†

James H. Earley,<sup>a</sup> Richard A. Bourne,<sup>a</sup> Michael J. Watson<sup>b</sup> and Martyn Poliakoff<sup>\*a</sup>

*n*-Butanol (BuOH) often has superior properties as a bio-fuel compared to ethanol (EtOH). However finding sustainable sources of BuOH is proving difficult. In this paper, direct production of BuOH from EtOH is compared over custom-synthesized six Cu catalysts, supported on different solid acids. These catalysts were tested in a continuous flow supercritical CO<sub>2</sub> (scCO<sub>2</sub>) reactor, and were found to catalyse the dehydrogenation, aldol condensation and hydrogenation steps of the so-called Guerbet reaction converting EtOH to BuOH. BuOH yields and selectivities were significantly different over the four catalysts. Cu on high surface area CeO<sub>2</sub> showed the best activity for BuOH formation, with yields above 30% achieved with good selectivity. In addition high pressure CO<sub>2</sub> is shown to have a positive effect on the reaction, possibly due to the redox cycle of Ce<sub>2</sub>O<sub>3</sub> and CeO<sub>2</sub>.

## Introduction

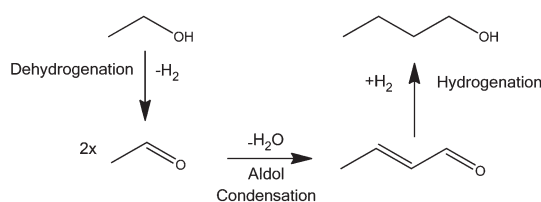
Interest in bio-fuels has increased considerably over recent years, particularly in view of concerns over climate change<sup>1</sup> and energy security.<sup>2</sup> One of the most common bio-fuels is EtOH which can be used as an additive to gasoline in unmodified gasoline engines,<sup>3</sup> or in high concentrations in more specialist engines. However EtOH has a number of problems as a fuel, including its miscibility with water, corrosion, and low energy content per unit volume compared to gasoline.

Therefore BuOH has advantages as a fuel, because it has a higher energy content than EtOH, lower water absorption and better miscibility with gasoline. Current gasoline engines need little or no modification to burn neat BuOH.<sup>4</sup> Furthermore unlike EtOH, BuOH can be transported without major problems in current gasoline pipelines.

Industrially, BuOH is manufactured *via* the high pressure OXO process,<sup>5</sup> where propylene is hydroformylated to butyraldehyde using *syn*-gas and a homogeneous rhodium catalyst; butyraldehyde is subsequently hydrogenated to BuOH. Alternatively BuOH can be produced from acetaldehyde *via* an aldol condensation, again followed by hydrogenation.<sup>6</sup>

BuOH can also be produced from EtOH *via* a sequence of steps collectively known as the Guerbet reaction. This one-pot

process involves conversion of a primary aliphatic alcohol into its β-alkylated dimeric alcohol with the loss of one equivalent of water *via* the aldol condensation and hydrogenation steps shown in Scheme 1. Koda *et al.* have used a homogeneous iridium catalyst in the presence of 1,7 octadiene and EtONa to promote the Guerbet reaction achieving turn over numbers (TONs) in excess of 1200 with 51% selectivity towards BuOH at 38% EtOH conversion.<sup>7</sup> Recently Dowson *et al.* reported a range of ruthenium centred catalysts.<sup>8</sup> In their system, a selectivity towards BuOH of 94% was achieved, but the conversion was only a little over 20%, with TONs only in the hundreds.<sup>8</sup> The Guerbet reaction has also been demonstrated successfully in batch processes for a variety of different heterogeneous systems, including Li-exchanged Zeolites,<sup>9</sup> MgO,<sup>10</sup> Mg/Al mixed metal oxides<sup>11</sup> and hydroxyapatites.<sup>12–14</sup> Many of these systems, however, suffer from poor conversions or selectivities and require temperatures above 400 °C and long reaction times.<sup>15</sup>



**Scheme 1** The Guerbet reaction: dehydrogenation of EtOH to acetaldehyde, followed by aldol condensation of acetaldehyde to form crotonaldehyde; finally BuOH is formed *via* hydrogenation of crotonaldehyde.

<sup>a</sup>School of Chemistry, The University of Nottingham, University Park, Nottingham, NG7 2RD, UK. E-mail: martyn.poliakoff@nottingham.ac.uk

<sup>b</sup>Johnson Matthey Technology Centre, POB 1, Belasis Ave, Billingham TS23 1LB, Cleveland, UK

† Electronic supplementary information (ESI) available. See DOI: 10.1039/c4gc00219a



This paper focuses on Cu catalysts and their use in the Guerbet reaction. In the dehydrogenation of EtOH over supported Cu catalysts, either EtOAc or acetaldehyde can be formed depending on the reaction conditions.<sup>16,17</sup> In these systems the Cu catalysts show good stability and activity at temperatures above 400 °C.<sup>17,18</sup> Cu has also been shown to successfully catalyse the hydrogenation of crotonaldehyde. In an attempt to synthesise BuOH, we have prepared catalysts by depositing Cu onto a range of supports capable of catalysing the aldol step. These include four acidic metal oxides (Al<sub>2</sub>O<sub>3</sub>, TiO<sub>2</sub>, silica/alumina SIRAL-40 from Sasol (Si/Al) and ZSM-5 zeolite) one high surface area (HSACeO<sub>2</sub>) and one regular surface area CeO<sub>2</sub>. In addition we have used supercritical CO<sub>2</sub> (scCO<sub>2</sub>), as the reaction medium because scCO<sub>2</sub> has been shown to improve selectivity and activity in several heterogeneously catalysed reactions, particularly in the present context, dehydrogenation,<sup>19</sup> aldol condensation<sup>20</sup> and hydrogenation.<sup>19,21</sup>

## Experimental

### Catalyst preparation

Cu(OAc)<sub>2</sub> was mixed with water at 70 °C and small amounts of concentrated HNO<sub>3</sub> were added in those cases where not all of Cu(OAc)<sub>2</sub> dissolved. Sufficient catalyst support was then poured into the solution whilst stirring to give a final Cu loading of 10% by weight. 4 M K<sub>2</sub>CO<sub>3</sub> was added until the solution had reached pH 9 and the suspension was then stirred for 1 h. The solid catalyst precursor was filtered under vacuum and washed with de-ionised water until the washings reached pH 7. The filtered solid was dried at 120 °C overnight and calcined in a furnace in air at 400 °C for 4 h.

### Catalyst characterisation

The catalysts were characterised using pXRD on a PANalytical X'pert Pro Multi-Purpose Diffractometer Fitted with a Cu K $\alpha$  X-ray source at The University of Nottingham. Nitrogen physisorption measurements were performed on Micromeritics ASAP 2420 and Micromeritics Tristar 3000 instruments using the ASTM method D 4222-83 at Johnson Matthey Billingham. The surface area was calculated by the Brunauer-Emmett-Teller (BET) method. The samples were outgassed at 140 °C with a nitrogen purge for 1 hour prior to isotherm measurements. TPR measurements were taken at Johnson Matthey Billingham using an AMI 5200 Altamira instrument. Prior to loading the sample, the material was ground to a sieve fraction of 100–250  $\mu$ m. 0.1 g of the sieved material was then loaded into a silica tube and the sample was then subjected to the following profile: firstly it was dried in 40 mL min<sup>-1</sup> of argon at 140 °C for 1 hour, then cooled to room temperature. The ramp for the TPR was room temperature to 1000 °C at 10 °C min<sup>-1</sup>, held for 15 minutes and cooled to room temperature; the gas flow was 40 mL min<sup>-1</sup> in 10% H<sub>2</sub>/Ar.

### Catalytic reactions

All experiments were carried out using a high pressure, automated continuous flow reactor with on-line GC analysis. The

reactor, described in detail previously,<sup>20</sup> is designed to record the effect on product yield of varying one reaction parameter (e.g. temperature, pressure, flow rate, *etc.*) at a time, (a diagram of the rig is included in the ESI†).

In a typical experiment, a tubular reactor (156 mm long  $\times$  3.525 mm internal diameter) was filled with catalyst and sealed into the apparatus. The catalysts were then reduced for 1 hour in a 5% H<sub>2</sub>/N<sub>2</sub> stream at 200 °C. After this, the reactor was cooled to 150 °C, the system pressure was set *via* the back pressure regulator, and the flows of EtOH and CO<sub>2</sub> were initiated. For all experiments, the flow rates were 1 mL min<sup>-1</sup> CO<sub>2</sub> and 0.05 mL min<sup>-1</sup> EtOH; this was consistent with an LHSV of 1.97 h<sup>-1</sup>. The temperature ramp for the catalytic reactions was 150–350 °C at 0.3 °C min<sup>-1</sup>.

The product stream was analysed with a Shimadzu GC-17A. The GC was fitted with a SPB-1701 column. Quantification was performed by integration of the peak areas; response factors and conversions were calculated by the internal normalisation method.<sup>22</sup> Direct sampling utilising an inline sample loop downstream of the reactor before depressurisation ensured that all volatile materials analysed.

Yields, conversions and selectivities were calculated as carbon yields, using the same method used by Ogo *et al.*<sup>15</sup> *via* the equation below where C wt is the% weight of carbon in the molecule.

$$\% \text{ EtOH conversion} = \frac{1 - \text{C wt of unreacted EtOH}}{\text{C wt of (products + unreacted EtOH)}} \times 100\%$$

$$\% \text{ Product yield} = \frac{\text{C wt of product}}{\text{C wt of specific product} + \text{C wt of unreacted EtOH}} \%$$

$$\% \text{ Product selectivity} = \frac{\% \text{ Product yield}}{\% \text{ EtOH conversion}} \times 100\%$$

Unfortunately turn over frequencies (TOFs) could not be calculated; due to the bi-functional nature of the catalysts it is not possible to define exactly what constitutes an active site *i.e.* Cu surface area relating to the hydrogenation/dehydrogenation reactions or the support that is catalysing the aldol step. In addition, for the Cu/CeO<sub>2</sub> catalysts, Cu surface area measurements could not be obtained because the standard procedure to measure Cu surface area is to use N<sub>2</sub>O frontal chromatography.<sup>23</sup> This method cannot be used Cu/CeO<sub>2</sub> catalysts as N<sub>2</sub>O is not only reduced by Cu but also by the CeO<sub>2</sub> support.

## Results and discussion

### Catalyst characterisation

The pXRD patterns for Cu/HSACeO<sub>2</sub> before and after reaction are shown in Fig. 1. The diffraction pattern for unreacted Cu/HSACeO<sub>2</sub> shows peaks at 27, 46 and 56 2 $\theta$ <sup>o</sup> corresponding to CeO<sub>2</sub> phases; these are broad indicating that the support is amorphous. Although the unreacted catalyst is almost certainly present as CuO, no peaks assignable to CuO are detected in the pattern suggesting that the crystallites are small and



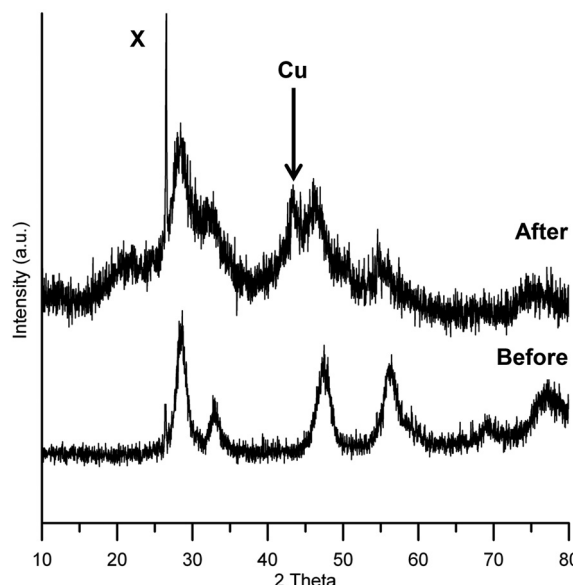


**Fig. 1** pXRD pattern of Cu/HSACeO<sub>2</sub> catalyst before and after reaction. Only one peak can be tentatively assigned to a Cu or CuO phase either before or after reduction. The pattern for the catalyst after reaction indicates a more amorphous structure possibly due to the formation of Ce<sub>2</sub>O<sub>3</sub> phases [The sharp peak at 26 2θ X is from the brass insert used in the sample holder].

highly dispersed. After reduction, the peaks of CeO<sub>2</sub> become broader, possibly as a result some of the CeO<sub>2</sub> having been reduced to Ce<sub>2</sub>O<sub>3</sub> reducing the crystallinity of the support. Only one small peak at 43 2θ can be assigned to a Cu metal phase, implying that, after reduction, the Cu crystallites have maintained their small size and good dispersion on the catalyst.

The Cu/HSACeO<sub>2</sub> had a comparatively large surface area and pore volume due to the nature of the CeO<sub>2</sub> support. The BET surface area of the catalyst was 178.3 m<sup>2</sup> g<sup>-1</sup>, the pore volume was [0.995 ads] cm<sup>3</sup> g<sup>-1</sup> 0.13 cm<sup>3</sup> g<sup>-1</sup> and the average pore diameter 30 Å.

Fig. 2 shows the TPR profile of the Cu/HSACeO<sub>2</sub> catalyst. Two peaks can be seen at 155 and 178 °C. In accordance with the previous literature,<sup>24,25</sup> the peak at 155 °C is assigned to CuO interacting strongly with the CeO<sub>2</sub> support and the peak at 178 °C to larger CuO particles with a weaker interaction with the CeO<sub>2</sub>.

### BuOH production

BuOH formation was observed over all six supported Cu catalysts. However the different catalysts showed significantly different selectivities and yields for BuOH, as shown in Fig. 3 and Table 1. It can be seen that both of the two CeO<sub>2</sub> supported catalysts performed better than the other three catalysts. Cu supported on the high surface area CeO<sub>2</sub> (Cu/HSACeO<sub>2</sub>) gave the best performance with 30% BuOH yield with a selectivity of 45%. This high yield was observed at 250 °C, a temperature low compared to those previously

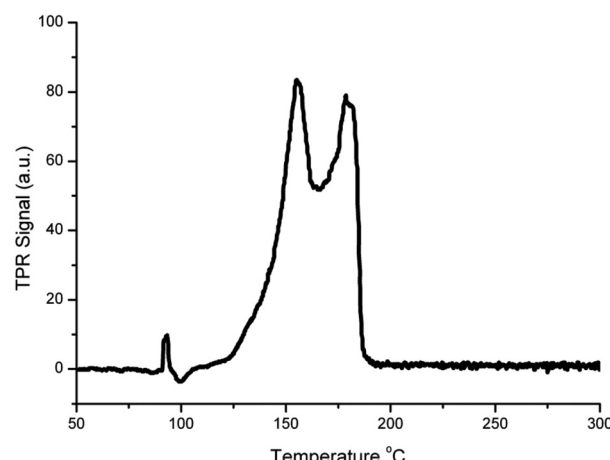


**Fig. 2** Results of temperature programmed reduction of the unreduced Cu/HSACeO<sub>2</sub> catalyst immediately following calcination; two well separated peaks can be seen at 155 and 178 °C, these two peaks are tentatively assigned to non-crystalline CuO interacting with CeO<sub>2</sub> and larger non-crystalline CuO associated with CeO<sub>2</sub> respectively.

reported for reactions over MgO and hydroxyapatite catalysts.<sup>10,12,14</sup> Over an MgO catalyst,<sup>10</sup> the maximum BuOH yield achieved was 18% and this was only achieved at the high temperature of 450 °C. Using hydroxyapatite based catalysts in a flow system, Ogo *et al.* reported good selectivity towards BuOH of 86.4% at 300 °C; the EtOH conversion, however, was only 11.3%. Using a Cu-Mg/Al mixed metal oxide catalyst in a batch system at 260 °C for 100 hours Marcu *et al.* achieved BuOH formation with 80% selectivity; however EtOH conversion was again poor at 8%.<sup>26</sup>

In the Cu/HSACeO<sub>2</sub> system here, high BuOH yields were maintained across the temperature range 200–350 °C. At 200 °C, the BuOH selectivity approached 70% whilst still giving a yield of *ca.* 20%. Good yields were also observed over the lower surface area CeO<sub>2</sub> catalyst (Cu/CeO<sub>2</sub>), which gave 17% BuOH yield with a selectivity of 29% at 313 °C. In addition, over the Cu/TiO<sub>2</sub> catalyst, significant BuOH formation was also observed, most notably with yields of around 13% at 270 °C.

Cu/CeO<sub>2</sub> catalysts have been widely reported for use in the Water Gas Shift reaction to generate H<sub>2</sub> and CO<sub>2</sub> from H<sub>2</sub>O and CO.<sup>24,27</sup> In these systems the Cu/CeO<sub>2</sub> catalysts show good stability at high reaction temperatures (300–450 °C) in a H<sub>2</sub> environment similar to the experiments presented here.<sup>28</sup> At these temperatures other supported Cu catalysts have been shown to deactivate quickly due to Cu sintering, which is a major cause of Cu catalyst deactivation.<sup>29</sup> There may be some stabilisation effects in the present system which may be why these Cu/CeO<sub>2</sub> catalysts are so active across the temperature range of the reaction.

With the other three catalysts, the BuOH yields were much lower; over Cu/Al<sub>2</sub>O<sub>3</sub>, BuOH was formed with a maximum yield of only 4% at 300 °C and a selectivity of just 5%. Cu/Si/Al, gave a maximum *n*-BuOH yield of 6% with 12% selectivity at



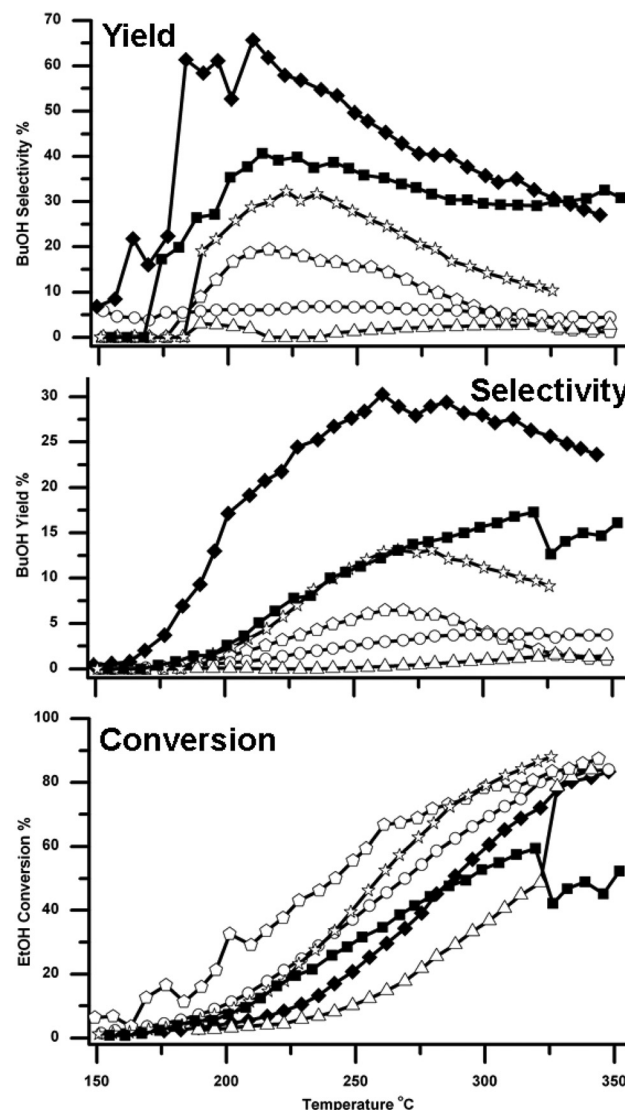


**Fig. 3** Traces showing how the yield of BuOH, selectivity to BuOH and conversion of EtOH, vary over the six different catalysts. The traces are marked as follows  $\circ$  Cu/Al<sub>2</sub>O<sub>3</sub>,  $\triangle$  Cu/ZSM-5 SAR-80,  $\star$  Cu/TiO<sub>2</sub>,  $\diamond$  Cu/Si/Al,  $\blacksquare$  Cu/CeO<sub>2</sub> and  $\blacklozenge$  Cu/HSA CeO<sub>2</sub>. Note that, although the yields varied, some BuOH was formed over all six catalysts.

270 °C. Cu/ZSM-5 was the poorest performing catalyst and gave a maximum yield of only 1%, coupled with the poorest EtOH conversion.

### Formation of other products

Fig. 4 shows how the formation of other products varies over the six catalysts. These data are important because the relative yields of these products help rationalize the observed activity of these catalysts for the production of BuOH. The additional products include acetaldehyde, EtOAc, diethyl ether (DEE) and higher molecular weight  $>C_4$  products, see Fig. 4A–H respectively.

Cu/ZSM-5 which gave the lowest yield of BuOH gives the highest yield of acetaldehyde and DEE. This suggests that (i) the ZSM-5 support was catalysing the dehydration of EtOH to DEE as has previously been reported,<sup>30</sup> and (ii) ZSM-5 was relatively inefficient at catalysing the aldol step in the Guerbet reaction. Therefore any acetaldehyde formed in the first step is not reacting further to form crotonaldehyde and subsequently BuOH. The Cu/Al<sub>2</sub>O<sub>3</sub> catalyst also gave rather low yields of BuOH, but it did give *high* yields of EtOAc and intermediate yields of DEE. This suggests that, over this catalyst, rather than catalysing the dehydrogenation to form acetaldehyde, the Cu/Al<sub>2</sub>O<sub>3</sub> support was promoting the dehydrogenation to EtOAc. The dehydrogenation of EtOH to EtOAc, has been well documented in the literature for a variety of supported Cu catalysts.<sup>16</sup> In addition to the formation of EtOAc the Al<sub>2</sub>O<sub>3</sub> is also catalysing the competing reaction to form DEE, observed previously,<sup>31</sup> but much less efficiently than Cu/ZSM-5.

The Cu/Si/Al catalyst led mainly to the formation of acetaldehyde, with a yield of 37% at 350 °C; there was also significant amounts of DEE and EtOAc formed. Again, the results suggest that this support has poor activity for catalysing the aldol condensation to crotonaldehyde.

The two CeO<sub>2</sub> supported catalysts generate only modest yields of acetaldehyde, EtOAc and DEE, but the Cu/HSACeO<sub>2</sub> catalyst produces significantly *greater* yields of higher molecular weight products (beyond C<sub>4</sub> alcohols and esters), which are likely to be formed through multiple aldol condensations

**Table 1** EtOH conversion and BuOH yield and selectivity over the supported Cu catalysts<sup>a</sup>

Catalyst	Temperature			260 °C			330 °C		
	190 °C			260 °C			330 °C		
	Yield (%)	Conv (%)	Sel (%)	Yield (%)	Conv (%)	Sel (%)	Yield (%)	Conv (%)	Sel (%)
Cu/Al <sub>2</sub> O <sub>3</sub>	0	7	6	3	48	7	3	82	5
Cu/ZSM-5	0	3	3	0	15	2	2	82	2
Cu/CeO <sub>2</sub>	2	5	27	13	39	35	14	47	31
Cu/HSACeO <sub>2</sub>	10	16	60	30	67	45	26	84	31
Cu/TiO <sub>2</sub>	1	6	19	13	53	25	9	9	10
Cu/Si/Al	1	3	9	6	30	14	2	78	2

<sup>a</sup> Yields, conversions and selectivities were calculated as carbon yields from GC data using the equations described in the Experimental section.



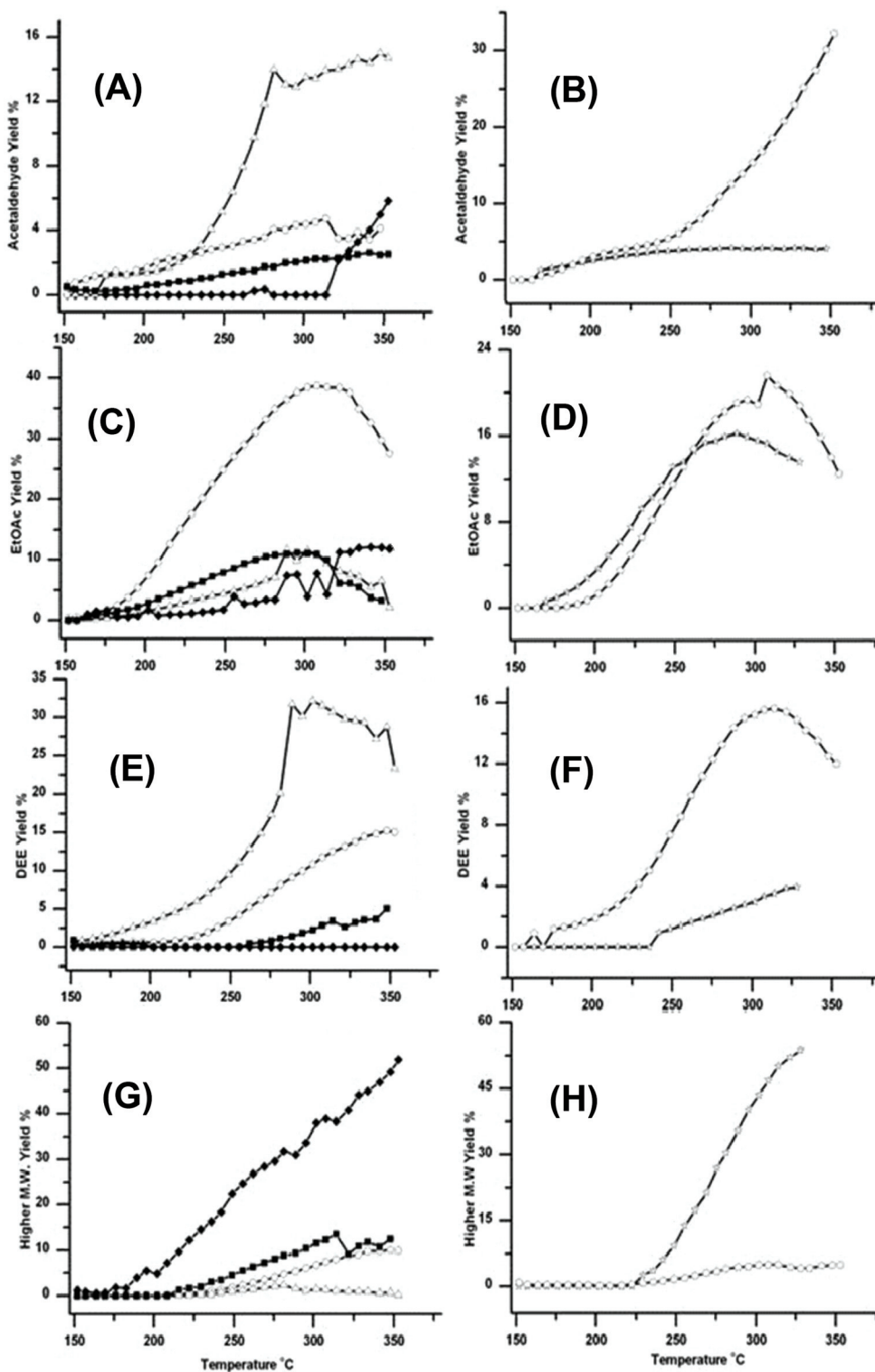
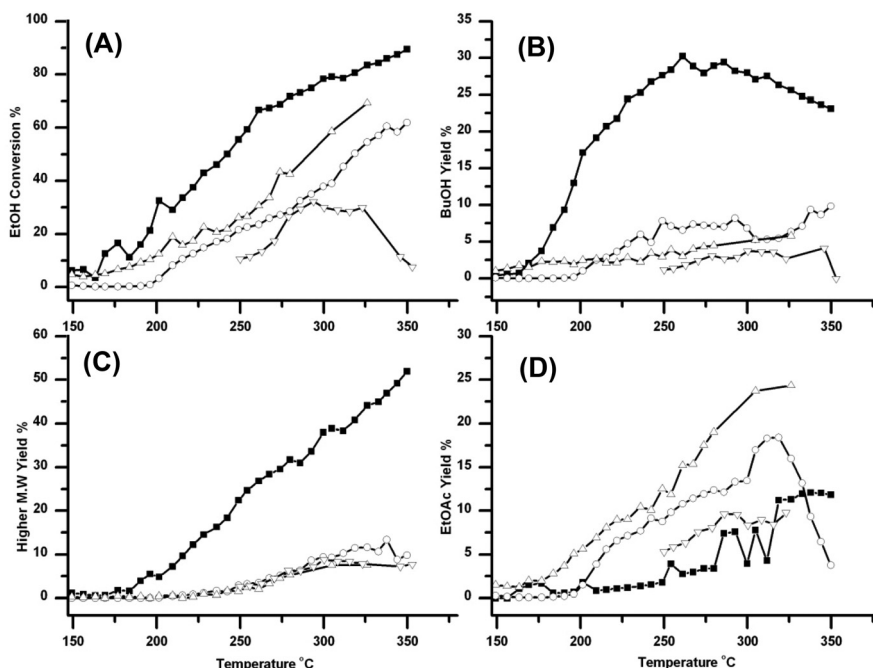


Fig. 4 Traces showing how the four different catalysts gave very different yields for Acetaldehyde (A)/(B) EtOAc (C)/(D) DEE (E)/(F) and Higher molecular weight products (G)/(H). The traces are marked as in Fig. 1;  $\circ$   $\text{Cu}/\text{Al}_2\text{O}_3$ ,  $\triangle$   $\text{Cu}/\text{ZSM-5 SAR-80}$ ,  $\star$   $\text{Cu}/\text{TiO}_2$ ,  $\square$   $\text{Cu}/\text{Si}/\text{Al}$ ,  $\blacksquare$   $\text{Cu}/\text{CeO}_2$  and  $\blacklozenge$   $\text{Cu}/\text{HSACeO}_2$ . DEE formation was greatest over  $\text{Cu}/\text{ZSM-5}$  and EtOAc greatest over  $\text{Cu}/\text{Al}_2\text{O}_3$ . However relatively large amounts of higher molecular weight products were formed over  $\text{Cu}/\text{HSACeO}_2$ ; these higher products are also potentially useful in fuels.





**Fig. 5** Summary of the effect of pressure and the presence of  $\text{CO}_2$  on the reaction over  $\text{Cu}/\text{HSACeO}_2$ . The traces show as follows (A) conversion of EtOH (B) yield of BuOH (C) yield of  $>\text{C}_4$  products and (D) yield of EtOAc. In each plot the points are labelled as follows: (without  $\text{CO}_2$ )  $\circ$  100 bar,  $\square$  30 bar,  $\triangle$  atmospheric pressure, and the result of  $\blacksquare$  100 bar  $\text{CO}_2$ . It can be seen that in the absence of  $\text{CO}_2$ , pressure has a negative effect on all four areas. By contrast the presence of  $\text{CO}_2$  enhances everything apart from the formation of EtOAc.

on the surface of the support. Production of these higher molecular weight products is not necessarily detrimental because, unlike EtOAc, DEE or acetaldehyde, they also have potential value in fuels.

The difference in activity between the two  $\text{CeO}_2$  supports can be attributed to the higher activity of the HSACeO<sub>2</sub> support for catalysing the aldol step compared to the lower surface area CeO<sub>2</sub> support. This difference is shown by the much higher yields of both BuOH and higher molecular weight products over the Cu/HSACeO<sub>2</sub> support. This is possibly due to the amorphous nature of the HSACeO<sub>2</sub> support leading to a greater number of acidic sites on the surface.

The Cu/TiO<sub>2</sub> catalyst was particularly active for the formation of higher molecular weight products with <55% yield at 325 °C. In addition EtOAc formation was also observed. These observations are consistent with the work of Luo *et al.*<sup>32</sup> who have studied the aldol reaction over Degussa® P25 TiO<sub>2</sub> and observed large amounts of chain propagation beyond crotonaldehyde through further aldol condensations.

#### Effect of $\text{CO}_2$ on formation of BuOH

All of the experiments described above were carried out in the presence of high pressure  $\text{CO}_2$ . Under such circumstances, one question always arises. What, if any, is the role of the  $\text{CO}_2$  in the reaction? In order to answer this question, the reaction was run in the absence of  $\text{CO}_2$  at atmospheric pressure, 30 and 100 bar, with the pressure being generated using the back pressure regulator. Fig. 5 summarises these results.

From the Figure it can be seen that (i) reasonable EtOH conversion occurs at atmospheric pressure in the absence of  $\text{CO}_2$  but the conversion drops dramatically as the pressure increases. This is quite surprising because, at constant mass flow of EtOH, the residence time will increase with pressure. (ii) The highest conversion is obtained in the presence of  $\text{CO}_2$ , and a pressure of  $\text{CO}_2$  has an effect on the product distribution. (iii) Relatively little BuOH is formed in the absence of  $\text{CO}_2$ . (iv) Pressure has little effect on the formation of higher esters, but the yield increases dramatically in the presence of  $\text{CO}_2$  and (v) in the absence of  $\text{CO}_2$  there is a relatively high yield of EtOAc at atmospheric pressure over the catalyst. This yield drops substantially as the pressure is increased; however 100 bar of  $\text{CO}_2$  has little further effect on yield of EtOAc.

In addition to the experiments performed in the absence of  $\text{CO}_2$ , the effect of the pressure of  $\text{CO}_2$  was investigated (the results are shown in the ESI Fig. 2†). The pressure of  $\text{CO}_2$  appears to have little effect on the reaction with yields and selectivities for *n*-BuOH similar at all of the pressures tested; 70, 100 and 180 bar. 100 bar is the most active system pressure with the best EtOH conversion and BuOH yield. Pressure and temperature will affect the density of the system and therefore the solvating properties of  $\text{CO}_2$  towards both products and reactants. Pressure is also likely to affect the equilibrium of the reaction; higher pressure should favour the aldol condensation reaction due to Le Chatelier's principle, although this appears to have had a small effect in this case.



The effect of  $\text{CO}_2$  has not been investigated further by us but the high rate of aldol condensation in the presence of  $\text{CO}_2$  could be due to  $\text{CO}_2$  and  $\text{H}_2\text{O}$  forming  $\text{H}_2\text{CO}_3$  and enhancing the acidity of the catalyst. In addition, the interaction of  $\text{CO}_2$  with  $\text{CeO}_2$  has been well documented in the literature,<sup>33</sup> because  $\text{CO}_2$  has been shown to re-oxidise  $\text{CeO}_{2-x}$  at low temperatures; this is of great importance catalytically, as oxygen from the bulk of  $\text{CeO}_2$  can migrate onto the supported metal particle and oxidise adsorbed species on the metal.<sup>34</sup> Thermodynamically the reaction,  $\text{Ce}_2\text{O}_3 + \text{CO}_2 \rightarrow 2 \text{CeO}_2 + \text{CO}$ , is favourable at 25 °C. Sharma *et al.*<sup>35</sup> demonstrated this phenomenon using a Pd/ $\text{CeO}_2$  catalyst with pulsed flow experiments at 350 °C. By alternating pulses of CO and  $\text{CO}_2$  they showed that CO is produced when  $\text{CO}_2$  is pulsed over reduced  $\text{CeO}_2$ . Staudt *et al.*<sup>36</sup> studied well-defined  $\text{CeO}_{2-x}$  films, supported on Cu (111) under UHV conditions, using resonant photoelectron spectroscopy to monitor the change in oxidation state of the  $\text{CeO}_2$  surface as a function of  $\text{CO}_2$  exposure and temperature. They discovered that oxidation of  $\text{CeO}_{2-x}$  by  $\text{CO}_2$  occurs, (i) at room temperature, (ii) without any supported metal co-catalysts and (iii) in the absence of surface hydroxyl groups or water.

This suggests that  $\text{CO}_2$  may indeed be playing an active role in the generation of aldol products (BuOH and higher molecular weight esters) in the  $\text{EtOH} + \text{Cu}/\text{HSACeO}_2$  experiments, particularly because these products are formed in only trace amounts the absence of  $\text{CO}_2$  in the reaction mixture. Therefore it is quite possible that  $\text{CO}_2$  is regenerating the  $\text{Ce}^{4+}$  species which are lost both during catalyst reduction and by reaction with the  $\text{H}_2$  that is generated in the dehydrogenation step, particularly because  $\text{Ce}^{4+}$  is active in the aldol condensation.<sup>37</sup> The pXRD pattern of the  $\text{Cu}/\text{HSACeO}_2$  catalyst after reduction (Fig. 1) shows that it has become more amorphous in nature, consistent with the formation of  $\text{Ce}_2\text{O}_3$  phases formed as a result of the hydrogen treatment.<sup>38</sup> Barteau *et al.* reduced  $\text{CeO}_2$  in pure hydrogen at 400 °C and observed large amounts of  $\text{Ce}^{3+}$  using XPS.<sup>39</sup> Le Normand *et al.* showed using X-ray absorption spectroscopy that during  $\text{CeO}_2$  reduction the amount of  $\text{Ce}^{3+}$  species formed was proportional to the surface area. The larger surface area  $\text{CeO}_2$  the higher the amount of reduction to  $\text{Ce}_2\text{O}_3$ . Addition of Cu to  $\text{CeO}_2$  is shown to reduce the redox potential of both Cu and  $\text{CeO}_2$ .<sup>40</sup> This has been exploited for water gas shift catalysis. Using  $\text{Cu}/\text{CeO}_2$  catalysts a complex relationship between Cu and the oxygen vacancies on ceria have been observed, this produces a catalyst that is much more active at lower temperatures.<sup>27</sup>

## Conclusions

In this paper, the continuous upgrading of EtOH to BuOH and higher esters has been demonstrated with better results both in terms of conversion and selectivity than in most of the recently reported batch or continuous reactions. The results presented here are probably the consequence of the increased activity of a  $\text{Cu}/\text{HSACeO}_2$  catalyst for the aldol condensation

step in the reaction sequence known as the Guerbet reaction. In addition, the presence of  $\text{CO}_2$  has a positive effect on the outcome of the reaction, possibly by enhancing surface acidity but more probably by re-oxidising the Ce without affecting the Cu. A secondary factor may be the smaller crystallite size of the Cu particles on the high surface area catalyst with a corresponding decreased tendency to sinter at higher temperatures. A more detailed engineering analysis would be required to decide whether high pressures of  $\text{CO}_2$  could be cost effective in a large scale commercial process to upgrade EtOH, but it is worth noting that fermentation to produce EtOH involves the co-production of  $\text{CO}_2$ . Overall the significance of this work is that it demonstrates that relatively high yields of BuOH can be obtained by upgrading EtOH using comparatively simple and uncomplicated catalysts.

## Acknowledgements

We thank Johnson Matthey, the EPSRC and the University of Nottingham for funding. We would also like to thank Mark Guyler, Richard Wilson and Peter Fields for their technical support at the University of Nottingham. We thank Michelle Gillespie at the Johnson Matthey for her help in catalyst synthesis and in the TPR and BET measurements.

## References

- 1 L. Ryan, F. Convery and S. Ferreira, *Energy Policy*, 2006, **34**, 3184–3194.
- 2 A. Demirbas, *Energy Convers. Manage.*, 2009, **50**, 2239–2249.
- 3 T. W. Patzek, *Crit. Rev. Plant Sci.*, 2004, **23**, 519–567.
- 4 P. Dürre, *Biotechnol. J.*, 2007, **2**, 1525–1534.
- 5 E. Billig and D. R. Bryant, in *Kirk-Othmer Encyclopedia of Chemical Technology*, John Wiley & Sons, Inc., 2000.
- 6 A. T. Nielsen and W. J. Houlihan, *Org. React.*, 1968, **1**, 1–438.
- 7 K. Koda, T. Matsu-ura, Y. Obora and Y. Ishii, *Chem. Lett.*, 2009, **38**, 838–839.
- 8 G. R. M. Dowson, M. F. Haddow, J. Lee, R. L. Wingad and D. F. Wass, *Angew. Chem., Int. Ed.*, 2013, **52**, 9005–9008.
- 9 C. Yang and Z. Y. Meng, *J. Catal.*, 1993, **142**, 37–44.
- 10 A. S. Ndou, N. Plint and N. J. Coville, *Appl. Catal., A*, 2003, **251**, 337–345.
- 11 S. Ordóñez, E. Díaz, M. León and L. Faba, *Catal. Today*, 2011, **167**, 71–76.
- 12 T. Tsuchida, S. Sakuma, T. Takeguchi and W. Ueda, *Ind. Eng. Chem. Res.*, 2006, **45**, 8634–8642.
- 13 T. Tsuchida, J. Kubo, T. Yoshioka, S. Sakuma, T. Takeguchi and W. Ueda, *J. Catal.*, 2008, **259**, 183–189.
- 14 S. Ogo, A. Onda and K. Yanagisawa, *Appl. Catal., A*, 2011, **402**, 188–195.
- 15 S. Ogo, A. Onda, Y. Iwasa, K. Hara, A. Fukuoka and K. Yanagisawa, *J. Catal.*, 2012, **296**, 24–30.

16 S. W. Colley, J. Tabatabaei, K. C. Waugh and M. A. Wood, *J. Catal.*, 2005, **236**, 21–33.

17 F.-W. Chang, H.-C. Yang, L. S. Roselin and W.-Y. Kuo, *Appl. Catal., A*, 2006, **304**, 30–39.

18 E. Santacesaria, G. Carotenuto, R. Tesser and M. Di Serio, *Chem. Eng. J.*, 2012, **179**, 209–220.

19 J. R. Hyde, P. Licence, D. Carter and M. Poliakoff, *Appl. Catal., A*, 2001, **222**, 119–131.

20 J. G. Stevens, R. A. Bourne and M. Poliakoff, *Green Chem.*, 2009, **11**, 409–416.

21 M. G. Hitzler, F. R. Smail, S. K. Ross and M. Poliakoff, *Org. Process Res. Dev.*, 1998, **2**, 137–146.

22 R. L. Grob and E. F. Barry, *Modern practice of gas chromatography*, Wiley, com, 2004.

23 G. C. Chinchen, C. M. Hay, H. D. Vandervell and K. C. Waugh, *J. Catal.*, 1987, **103**, 79–86.

24 X.-c. Zheng, X.-l. Zhang, X.-y. Wang and S.-h. Wu, *React. Kinet. Catal. Lett.*, 2007, **92**, 195–203.

25 L. Kundakovic and M. Flytzani-Stephanopoulos, *J. Catal.*, 1998, **179**, 203–221.

26 I.-C. Marcu, D. Tichit, F. Fajula and N. Tanchoux, *Catal. Today*, 2009, **147**, 231–238.

27 X. Wang, J. A. Rodriguez, J. C. Hanson, D. Gamarra, A. Martínez-Arias and M. Fernández-García, *J. Phys. Chem. B*, 2005, **110**, 428–434.

28 X. Qi and M. Flytzani-Stephanopoulos, *Ind. Eng. Chem. Res.*, 2004, **43**, 3055–3062.

29 M. Twigg and M. Spencer, *Top. Catal.*, 2003, **22**, 191–203.

30 I. Takahara, M. Saito, M. Inaba and K. Murata, *Catal. Lett.*, 2005, **105**, 249–252.

31 S. Golay, R. Doepper and A. Renken, *Appl. Catal., A*, 1998, **172**, 97–106.

32 S. Luo and J. Falconer, *Catal. Lett.*, 1999, **57**, 89–93.

33 C. Li, Y. Sakata, T. Arai, K. Domen, K.-i. Maruya and T. Onishi, *J. Chem. Soc., Faraday Trans. 1*, 1989, **85**, 929–943.

34 C. Bozo, N. Guilhaume and J.-M. Herrmann, *J. Catal.*, 2001, **203**, 393–406.

35 S. Sharma, S. Hilaire, J. M. Vohs, R. J. Gorte and H. W. Jen, *J. Catal.*, 2000, **190**, 199–204.

36 T. Staudt, Y. Lykhach, N. Tsud, T. Skála, K. C. Prince, V. Matolín and J. Libuda, *J. Catal.*, 2010, **275**, 181–185.

37 M. I. Zaki, M. A. Hasan and L. Pasupulety, *Langmuir*, 2001, **17**, 768–774.

38 P. Bera, S. Mitra, S. Sampath and M. S. Hegde, *Chem. Commun.*, 2001, 927–928.

39 H. Idriss, C. Diagne, J. P. Hindermann, A. Kiennemann and M. A. Barteau, *J. Catal.*, 1995, **155**, 219–237.

40 J. El Fallah, S. Boujana, H. Dexpert, A. Kiennemann, J. Majerus, O. Touret, F. Villain and F. Le Normand, *J. Phys. Chem.*, 1994, **98**, 5522–5533.

